

How Anomalous Resistivity Accelerates Magnetic Reconnection

H. Che

*University of Maryland, College Park, MD, 20742, USA and
 NASA Goddard Space Flight Center, Greenbelt, MD, 20771,
 USA*

(Dated: 24 March 2024)

Whether Turbulence-induced anomalous resistivity (AR) can facilitate a fast magnetic reconnection in collisionless plasma is a subject of active debate for decades. A particularly difficult problem in experimental and numerical simulation studies of the problem is how to distinguish the effects of AR from those originating from Hall-effect and other non-turbulent processes in the generalized Ohm's. In this paper, using particle-in-cell simulations, we present a case study of how AR produced by Buneman Instability accelerates magnetic reconnection. We first show that in a thin current layer, the AR produced by Buneman instability spontaneously breaks the magnetic field lines and causes impulsive fast non-Hall magnetic reconnection on electron-scales with a rate reaching $0.6 V_A$. However, the electron-scale magnetic reconnection is not a necessary condition for the dissipation of magnetic energy, but rather a result of the inhomogeneity of the AR. On the other hand, the inhomogeneous drag arising from a Buneman instability driven by the intense electron beams in a 3D ion-scale magnetic reconnection can drive electron-scale magnetic reconnections at the x-line. The electron-scale reconnections play an essential role in accelerating the ion-scale magnetic reconnection with a rate two times faster than the non-turbulent Hall-dominated 2.5D ion-scale magnetic reconnection. The ion-scale reconnection rate is enhanced around the x-line, and the coupling between the AR carried out by the reconnection outflow and the Hall effect leads to the breaking of the symmetric structure of the ion diffusion region and the enhancement of the outward Poynting flux.

I. INTRODUCTION

In the Earth's magnetosphere^{1–5} and solar and stellar atmospheres^{6–8}, plasma heating commonly occurs in current sheets of various scales. Different types of micro-instabilities, including both electrostatic(ES) and electromagnetic(EM) instabilities, can be triggered in the current sheets. Some can lead to the merging and rearranging of oppositely directed magnetic field lines and the bursty releasing of magnetic energy, a process known as magnetic reconnection.

In magnetic reconnections, the breaking of magnetic field lines requires the ideal magnetohydrodynamics (MHD) frozen-in condition $\mathbf{E} + \mathbf{U} \times \mathbf{B} = 0$ to be broken. In resistive MHD theory, e.g. the established Sweet-Parker model⁹, it is the collisional resistivity η that breaks the frozen-in condition, and the Ohm's law assumes the well known form $\mathbf{E} + \mathbf{U} \times \mathbf{B} = \eta \mathbf{j}$. However, the collisional resistivity of space plasma is usually too low to facility a sufficiently fast Sweet-Parker magnetic reconnection to explain the observed magnetic energy release in solar flares and magnetospheric substorms.

An alternative model, Hall-MHD magnetic reconnection, includes the two-fluid effects which become important as the current sheet becomes so thin that ions and electrons decouple from each other. The Ohm's law is replaced by the generalized Ohm's law – the first electron moment of Vlasov equation^{10,11}:

$$\mathbf{E} + \frac{1}{c} \mathbf{U}_i \times \mathbf{B} = -\frac{m_e}{e} (\partial_t \mathbf{U}_e + \mathbf{U}_e \nabla \cdot \mathbf{U}_e) + \frac{1}{en_e c} \mathbf{j} \times \mathbf{B} - \frac{1}{en_e} \nabla \cdot \mathbb{P}_e - \eta \mathbf{j}_e, \quad (1)$$

where we have split $\mathbf{U}_e \times \mathbf{B}/c \equiv (\mathbf{U}_i - \mathbf{j}/en_e) \times \mathbf{B}/c$, assuming $n_e \approx n_i$. The term $\mathbf{j} \times \mathbf{B}/c$ is called the Hall term¹². Beside the electron Joule heating $\eta \mathbf{j}_e$, the generalized Ohm's law presents more terms that can break the frozen-in condition, including the gradient of electron pressure \mathbb{P}_e and the electron inertial terms (acceleration $\partial_t \mathbf{U}_e$ and convective momentum $\mathbf{U}_e \nabla \cdot \mathbf{U}_e$). The Hall term increases as the spatial scale approaches the ion inertial length $d_i = c/\omega_{pi}$ ($\omega_{pi} = \sqrt{m_i/4\pi e^2 n_e}$) but decreases as the spatial scale decreases to the electron inertial length $d_e = c/\omega_{pe}$. The Hall term becomes zero at the x-point and thus it can not break magnetic field lines. The inertia and pressure terms are important on electron scales^{10,13–15}. Numerical simulations^{10,16,17} show that Hall-reconnection is dramatically faster than Sweet-Parker reconnection, and its reconnection rate is universal and independent of the mechanism that breaks the field lines. However, observations of solar flares found that the reconnection rate in solar flares, estimated by the time-change of magnetic flux

around magnetic null-points, can reach 0.5-0.6 V_A ¹⁸, much higher than the maximum steady anti-parallel Hall-reconnection rate 0.2 V_A . Since solar flare magnetic reconnections mostly have strong guide magnetic field, and experiments¹⁹ and simulations^{20,21} show that the reconnection rate of guide field reconnection is lower than the anti-parallel reconnection rate, the discrepancy between theory and observation is more severe than it appears. New *in-situ* *Magnetospheric Multiscale* (MMS) observations of asymmetric magnetopause reconnection also find that the observed reconnection rate is 0.1 V_A , much higher than asymmetric Hall-reconnection rate which is a small fraction of 0.1 V_A ²².

It's not surprising that the inconsistency exists between observations and the Hall-magnetic reconnection model. The theory of Hall-reconnection is based on the steady fluid model whereas the observations of solar flares and magnetospheric substorms show that magnetic reconnection are generally impulsive and turbulent²³⁻²⁶. While the theory of collisional magnetic reconnection is well established, turbulent magnetic reconnection which involves wave-wave and wave-particle interactions on a broad range of spatial and time scales is poorly understood. What is known is that the turbulence effects such as anomalous resistivity (AR) and anomalous viscosity (AV) can dramatically influence the energy dissipation and convective momentum transport. Thus the generalized Ohm's law in Eq. (1) needs to be modified for turbulent reconnection²⁰:

$$\langle \mathbf{E} \rangle + \langle \mathbf{U}_e \rangle \times \langle \mathbf{B} \rangle / c = \mathbf{D}_e + \nabla_{\perp} \cdot \mathbf{\Xi}_e - \frac{m_e}{e} (\partial_t \langle \mathbf{U}_e \rangle + \langle \mathbf{U}_e \partial \cdot \mathbf{U}_e \rangle) - \frac{1}{e \langle n_e \rangle} \partial \cdot \langle \mathbb{P}_e \rangle. \quad (2)$$

where $\mathbf{D}_e \equiv -\langle \delta n_e \delta \mathbf{E} \rangle / \langle n_e \rangle$ is the drag, i.e. AR, $\mathbf{\Xi}_e \equiv -\langle \delta \mathbf{p}_e (\delta \mathbf{U}_e - e \delta \mathbf{A} / m_e c) \rangle / e \langle n_e \rangle$ is AV, $\mathbf{p}_e = n_e \mathbf{U}_e$, and \mathbf{A} is the magnetic vector potential. $\langle \rangle$ denotes the ensemble average of the turbulence properties.

AR²⁷ induced by ES instabilities, arising from ion-electron drag, and AV²⁸ induced by EM instabilities, arising from anomalous momentum transport, are widely believed to be responsible for fast magnetic reconnection in collisionless plasma²⁹⁻³³. But how AR and AV affect the dynamics of magnetic reconnection is unclear. Especially, the question of whether or not AR can facilitates fast magnetic reconnection is a subject of debate for nearly half a century^{20,34-41}.

High spatial resolution observations of the generalized Ohm's Law (Eq. 1) in the magnetopause reconnection from *MMS* provide direct evidence that the AR associated with electron heating around the x-line is not negligible²². Many *MMS* observations discover

coherent electrostatic structures and electron heating in electron diffusion regions, implying that ES instabilities are common in reconnections^{22,42–46}. In addition, Magnetic Reconnection Experiment (MRX) suggested that AR may be able to facilitate a fast Sweet-Parker-like magnetic reconnection^{38,47}. Thus it is important to understand the role of AR in magnetic reconnection.

In this paper, we concentrate on AR induced by Buneman instability in a strong guide-field reconnection. Buneman instability is triggered due to the intense electron beams developed at the x-line once the electron beam velocity is larger than the electron thermal velocity²⁷, and is common in magnetic reconnection^{29,40,48–50}. Recent *MMS* observations of magnetospheric reconnection discovered that Buneman instability can efficiently brake the electron jet at the exhaust of the diffusion region⁴². Electron holes driven by Buneman instability are often discovered to associate with current sheets or reconnections in magnetosphere^{44,51–55}. Intense electron beams are also found to associate with solar flares⁵⁶

We focus on the role of AR produced by Buneman instability in the early stage of magnetic reconnections. Given that Buneman instability is triggered when the current sheet becomes very thin, we first investigate AR induced by Buneman instability in a thin current layer in 3D, and show how the instability drives a fast spontaneous unsteady electron-scale magnetic line annihilation as the magnetic energy is dissipated. The electron-scale magnetic reconnection is not affected by the Hall effect and is much faster than Hall-reconnection. The topology change of the magnetic field is caused by the inhomogeneous drag rather than the magnetic energy dissipation. We then look at magnetic reconnections in which intense electron beam causes Buneman instability to occur at the x-line. We find that Buneman induced electron-scale magnetic reconnections occur at the x-line in a 3D reconnection. The electron-scale magnetic reconnection breaks the field lines, enhances the reconnection rate in the electron diffusion region, and widens the opening angle of the exhaust of the ion diffusion region—implying that the AR can add to the Hall-effect in shaping the geometry of the reconnection. These effects cause the reconnection with Buneman turbulence induced AR to be faster than non-turbulent Hall-reconnection.

II. SIMULATIONS AND ANALYSIS

Four PIC simulations using P3D code⁵⁷ are used in this paper, including Buneman instability simulations in a thin current layer in 2.5D and 3D and magnetic reconnection simulations also in 2.5D and 3D.

The initialization of these simulations are similar. The differences are 1) the width of the initial current sheet in Buneman instability simulation and magnetic reconnection simulations are of electron and ion inertial length scales, respectively; and 2) no initial perturbation is applied in the Buneman instability simulation so that the Buneman instability can develop well before magnetic reconnection starts.

The initial magnetic field has a force-free configuration, with $B_x/B_0 = \tanh[(y - L_y/2)/w_0]$, where w_0 and L_y are the half-width of the initial current sheet and the box size in y -direction, respectively. The guide magnetic field $B_g^2 = B_{z,0}^2 = B^2 - B_x^2$ is chosen so that $|B| \equiv \sqrt{26}B_0$. We choose $w_0 = d_e$ in the Buneman instability simulations and $w_0 = 0.5d_i$ in magnetic reconnection simulations. Simulations use periodic boundary conditions in the x and z directions, and a conducting boundary condition in the y direction. The initial plasma temperature is isotropic and uniform, with $T_{e0} = T_{i0} = 0.04m_i c_{A0}^2$, where $c_{A0} = B_0/(4\pi n_0 m_i)^{1/2}$ is the asymptotic ion Alfvén wave speed. A mass ratio $m_i/m_e = 100$ is used in all simulations. The force-free condition requires $\mathbf{j}_e \times \mathbf{B} = 0$, thus initially $j_{ex}/j_{ez} = B_x/B_z$.

The domain of 3D simulation of Buneman instability has dimensions $L_x \times L_y \times L_z = 1d_i \times 1d_i \times 2d_i$. The initial electron drift velocity is $v_{de} \sim 9c_{A0} \sim 3v_{tez,0}$, which is large enough to trigger electrostatic Buneman instability. The initial ion drift is about $0.9 v_{A0} \ll v_{tez,0}$, and can be neglected. The total simulation time is $\omega_{pe,0}t = 160$ where $\omega_{pe,0} \equiv (4\pi n_e e^2/m_e)^{1/2}$. The same initialization is used in the corresponding 2.5D simulation except that only 1 cell is used in the x -direction.

The 2.5D PIC Buneman instability simulation is carried out with the same parameters as those of the 3D simulation. The 2.5D simulation is in the y - z plane in which the waves of Buneman instability propagate along z and form 2.5D electron holes in the y - z plane.

The domain of 3D magnetic reconnection has dimensions $L_x \times L_y \times L_z = 4d_i \times 2d_i \times 8d_i$. The total simulation time is $\Omega_i t = 4$, where Ω_i is the ion gyro-frequency and $\omega_{pe,0}/\Omega_i = 200$. The corresponding 2.5D reconnection domain is $L_x \times L_y = 4d_i \times 2d_i$.

A. 3D Buneman Instability and the Spontaneous Fast Electron-Scale magnetic reconnection

The 3D PIC Buneman instability simulation shows that a Buneman instability is driven along the magnetic field (which is close to the z -direction) at $\omega_{pe,0}t \sim 40$ with the initial growth rate $\sqrt{3}/2(m_e/2m_i)^{1/3}\omega_{pe,0} \sim 0.1\omega_{pe,0}$, consistent with the linear growth rate of Buneman instability in cold plasma. The electric fluctuations $\langle \delta E_z^2 \rangle^{1/2}$ generated by the Buneman instability reaches its peak at $\omega_{pe,0}t \sim 70$ and then decay and saturate at $\omega_{pe,0}t \sim 160$. As the magnitude of electric fluctuations become large enough to trap electrons and form electron holes with electric potential satisfying $\phi > kT_e$, the Buneman instability enters the nonlinear stage and the growth rate decreases due to thermal effects⁵⁸. The fast adiabatic energy exchange between the electron holes and the trapped electrons causes rapid phase mixing and heating, leading to the decay of the waves and the de-trapping of electrons until the saturation of the Buneman turbulence when the electron holes break up⁵⁸. Previous study⁵⁹ showed that the kinetic energy of current sheets is dissipated by AR in the form of drag \mathbf{D}_e , and at the same time the current-carried magnetic energy is also dissipated. Can AR break the magnetic field lines is a question naturally raised.

We first take a closer look at the magnetic field after the Buneman instability occurs at $\omega_{pe,0}t \sim 40$. With the onset of Buneman instability, electron-scale magnetic reconnections appear at different locations along the mid-plane of the current sheet, as shown in the supplementary movie. Examples of the magnetic field lines at $\omega_{pe,0}t = 48, 60$ are shown in Fig. 1. Magnetic field perpendicular to the current sheet B_y , which was originally zero, is generated at $x = 0.7d_i$ and forms an x-line at $\omega_{pe,0}t = 60$ – a clear manifestation of topological change of the magnetic fields. As a result of the microscopic magnetic reconnection, an inductive electric field $\langle E_z \rangle$ is also produced. The corresponding drag $\langle \delta n_e \delta E_z \rangle$ becomes much stronger while the corresponding $\langle j_{ez} \rangle$ becomes much weaker due to the dissipation. The corresponding localized intense electric field E_z and the electron density fluctuations in the mid-plane $x - z$ create the intense drag.

An important feature of the electron-scale magnetic reconnection is that contrary to ion-scale reconnection, contribution from Hall-effect is negligible. In Hall-reconnections the Hall effect generates an out-of-plane *Hall magnetic field*^{60,61}, which is thought to be brought up by Hall-induced whistler wave in anti-parallel reconnection, or by kinetic Alfvén wave in guide-

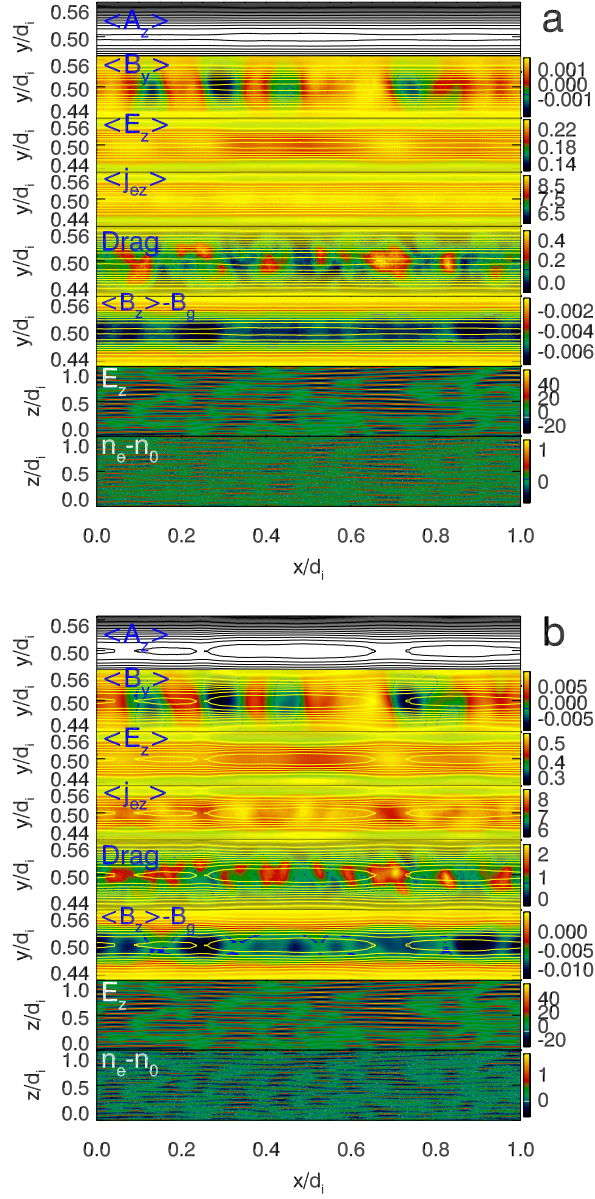


FIG. 1. (a): Quantities at $\omega_{pe,0}t = 48$ in the current sheet simulation when the Buneman instability occurs. (b): The same quantities as in (a) but at $\omega_{pe,0}t = 60$ when the Buneman instability reaches its peak. $\langle A_z \rangle$ is the z-component of the magnetic field vector potential. Please see the supplementary movie for the electron-scale magnetic reconnection. $\langle \rangle$ denotes the spatial average over z-direction in the simulation. E_z and electron density fluctuations $n_e - n_0$ are shown in the mid-plane x-z of the current sheet.

field reconnection^{62,63}. Hall field has a quadrupole structure in anti-parallel reconnections⁶⁴, and the quadrupole is distorted in guide-field reconnections^{21,65}. Such a quadrupole Hall field is clearly absent in the simulation as shown in the out-of-plane magnetic field $\langle B_z \rangle - B_g$ produced during the Buneman instability in Fig. 1. What we observe is a very small decrease of B_z caused by the dissipation of j_{ex} ($\ll j_{ez}$).

How does the drag drive electron-scale magnetic reconnection during Buneman instability? In an early paper⁵⁹(C14 hereafter) we found when $\Xi_e = 0$, the Ohm's Law (Eq. 2) can be split into two equations:

$$\langle E_z \rangle = -\frac{m_e}{e} \partial_t \langle U_{ez} \rangle + \langle D_{ez} \rangle, \quad (3)$$

$$E_z^{wv} = E_z - \langle E_z \rangle = -\frac{m_e}{e} U_{ez} \partial_z U_{ez} - \frac{1}{e \langle n_e \rangle} \partial_z P_{ezz}, \quad (4)$$

where E_z^{wv} is the Buneman instability generated coherent electric field, $\langle E_z \rangle$ is the mean electric field, and $E_z = E_z^{wv} + \langle E_z \rangle$. Buneman instability produces electron holes along z near the mid-plane of the current sheets. The z -average $\langle E_z \rangle$ cancels out local effects of the electron holes since $\langle E_z^{wv} \rangle = 0$, and only the large-scale inductive electric field produced by electron-scale magnetic reconnection is left. The inductive electric field is related to the magnetic vector potential by $\langle E_z \rangle = -\partial_t \langle A_z \rangle / c$ using Coulomb gauge. Eq. 3 establishes the relation between reconnection rate and the drag and the dissipation of kinetic energy, while Eq. 4 describes a differential Bernoulli-like relation satisfied inside electron holes—the macroscopic effects caused by microscopic anomalous momentum transports that supports the growth of Buneman instability.

An important distinction between the AR facilitated electron-scale magnetic reconnection and Hall-reconnection is the reconnection rate $\langle E_z \rangle$. The reconnection rate from our simulation is $\sim 0.6 B_0 v_{A,0} / c$ at the peak, much larger than the maximum rate of 0.1-0.2 in anti-parallel Hall-reconnections¹⁰. The maximum rate for Hall-reconnections with guide field is generally lower than the 0.1-0.2 value.

The wave couplings of Buneman instability causes the drag to be non-uniform within the current sheet and such non-uniformity determines the topology of the magnetic field. In Fig. 1, both the reconnection electric field and the drag appear "clumpy" in the x -direction and form "wave-packets" with scale $\sim 0.1 d_i$. Combining the relation $\langle E_z \rangle = -\partial_t \langle A_z \rangle / c$ and

the Ampère's law, we obtain the equation of $\langle A_z \rangle$ around the mid-plane of the current sheet:

$$\partial^2 \langle A_z \rangle - \frac{1}{c^2} \partial_t^2 \langle A_z \rangle + \frac{4\pi}{c} \langle j_{ez} \rangle = 0, \quad (5)$$

where $\partial^2 \equiv \partial_x^2 + \partial_y^2$, and we have neglected the contribution from j_{ex} which is much smaller than j_{ez} . Eq.5 is a standard d'Alembert equation. The solution is

$$\langle A_z(\mathbf{x}) \rangle = \frac{1}{c} \int \frac{\langle j_{ez} \rangle(\mathbf{x}', t - r/c)}{r} dx dy, \quad (6)$$

where $\mathbf{r} = \mathbf{x}' - \mathbf{x}$. The magnetic topology is determined by the spatial distribution of current sheets which is coupled to the drag by

$$\frac{1}{c} \partial_t \langle A_z(\mathbf{x}) \rangle = \frac{m_e}{e} \partial_t \langle j_{ez}/n_e \rangle - D_{ez}. \quad (7)$$

The magnetic vector potential is the near field solution of d'Alembert equation and the magnetic field is a static field, and its change in the xy plane describes the change of magnetic field topology $B_x = -\partial_y A_z$ and $B_y = -\partial_x A_z$.

It should be noted that the electron-scale magnetic reconnection is not necessary for the dissipation of magnetic energy. To illustrate this point, we conduct a 2.5D Buneman instability simulation in the yz plane and no electron-scale magnetic reconnections can develop in this setting.

Fig. 2 shows the electric field E_z at $\omega_{pe,0}t = 60$. Electron holes form along the z-direction and the drag produced by the electron holes can dissipate the kinetic energy and the associated magnetic energy. At the same time, electron heating is produced in both the parallel and perpendicular directions of the magnetic field. The time evolutions of electron kinetic, magnetic energy and pressure are shown in Fig. 3, which are nearly identical to the evolutions of these quantities in the 3D simulation reported in C14. It is clear that the inductive electric field is produced due to the fast decrease of magnetic field (Fig. 4) whose time evolution is similar to that in the 3D simulation. In the 2.5D simulation no electron-scale magnetic reconnection develops, $\langle B_y \rangle$ is zero although B_y oscillates (Fig. 4).

To summarize, electron-scale magnetic reconnection is produced by the inhomogeneity of drag along the magnetic field which leads to inhomogeneous magnetic energy dissipation. The reconnection rate is significantly higher than Hall-reconnection rate. With the new insight of electron-scale magnetic reconnection, we can look into the role of AR in larger scale magnetic reconnections.

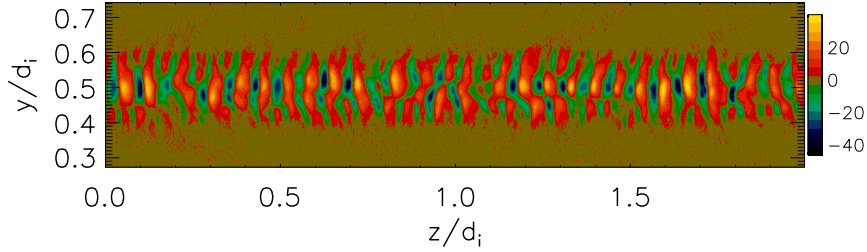


FIG. 2. E_z in the 2.5D Buneman instability simulation at $\omega_{pe,0}t = 60$, when strong electron holes are developed.

B. How does Anomalous Resistivity Accelerate Ion-Scale Magnetic Reconnection?

The Buneman instability grows along the current sheet perpendicular to the reconnection plane, thus the instability cannot develop in the 2.5D simulation. Comparing the 2.5D and 3D simulations allows us to clearly demonstrate the effects of turbulence generated by the Buneman instability. In the 3D ion-scale magnetic reconnection simulation, turbulence driven by an ES Buneman instability and an EM electron velocity shear instability at x-line makes the magnetic reconnection significantly faster than the non-turbulent 2.5D reconnection (the details can be found in a previous paper²⁰ which we refer as CDS hereafter). The Buneman instability produces electron holes in the early stage for a brief period around $\Omega_{i0}t \sim 0.3$ (Ω_{i0} is the asymptotic ion gyro-frequency) while the electron velocity shear instability starts to widen the current sheet and entails the filamentary structures at later stage. Close examination of Eq. (2) in CDS shows that before the onset of Buneman instability, at the x-line the reconnection electric field $\langle E_z \rangle$ (reconnection is in the xy -plane) is fully sup-

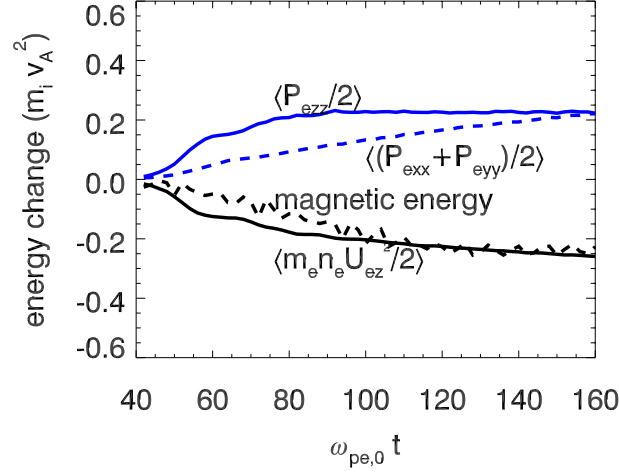


FIG. 3. The time evolution of energy change in 2.5D Buneman instability simulation. Black solid: kinetic energy of electron beams; black dashed line: magnetic energy. Blue solid line: electron parallel thermal energy; blue dashed line: perpendicular thermal energy.

ported by the electron inertia. As the Buneman instability is triggered, the increasing drag reduces the electron acceleration, and eventually the drag becomes comparable to the electron inertia. Later the growth of electron velocity shear instability surpasses the Buneman instability and become dominant. The AV induced by the anomalous momentum transport grows fast and quickly fully supports the reconnection. As the reconnection reaches its steady state, the repeating occurrences of electron velocity shear instability continuously maintain the fast reconnection. How does the drag/AR impacts the magnetic reconnection? We need to answer two separate questions: 1) how does the drag affect the reconnection at the x-line? 2) can the drag affect the geometry of the ion diffusion region, or the geometry is only determined by the Hall term as previously believed?

First we show in Fig.5 the electron current density j_{ez} in 2.5D reconnection and $\langle j_{ez} \rangle$ in 3D reconnection when the Buneman instability begins at $\Omega_{i0}t = 3$, and when it reaches its peak at $\Omega_{i0}t = 3.4$. The Buneman instability is in the z-direction and affects the width of

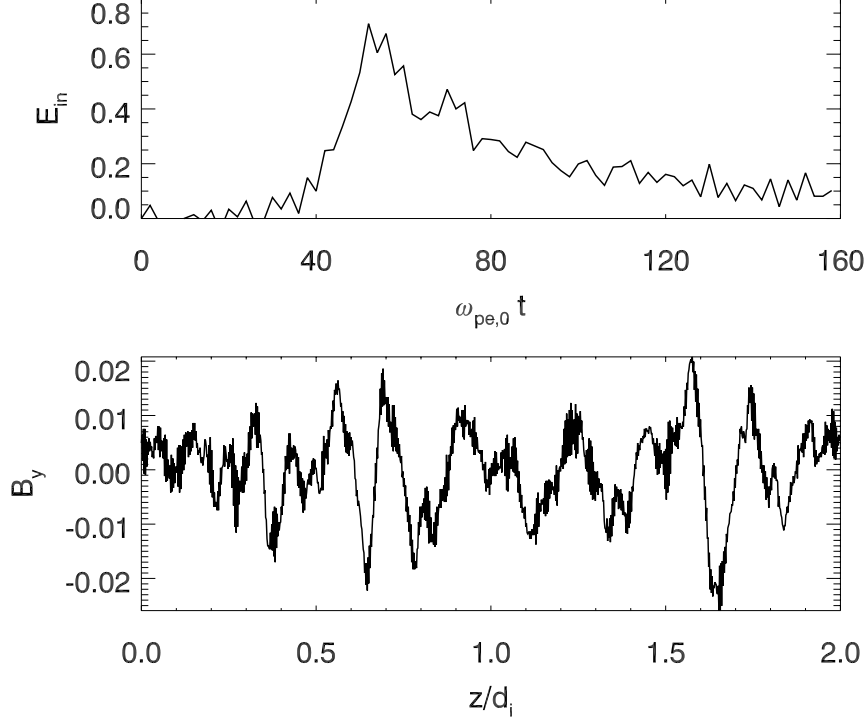


FIG. 4. Top panel: The time evolution of inductive electric field $\langle E_z \rangle$ in the 2.5D Buneman instability simulation. Bottom panel: The B_y generated along z at $\Omega_{pe,0} = 60$ in the same simulation.

the current sheet only slightly, but the length of the current sheet in the reconnection plane is much longer in 3D than in 2.5D reconnection, implying that the AR (drag) induced by the Buneman instability could play a similar role as collisional resistivity. This is because the plasma outflow can bring electron holes out while new holes are produced near the x-line. We show the drag D_{ez} at $\Omega_{i0}t = 3, 3.4$ at in xy plane in Fig.5. We can see that the drag spread in both x and y direction, but over time the spatial scale of the region where the drag is strong significantly increases in the x -direction, enabling the drag to extend from the x-point to the ion diffusion region. As we expect, the drag is inhomogeneous along the x -direction.

To understand how the Buneman instability enhances the reconnection electric field $\langle E_z \rangle$, we show $\langle E_z \rangle$ in the xy plane at $\omega_{pe,0}t = 680$ ($\Omega_{i0}t = 3.4$) in both the 3D and 2.5D simulations in Fig.6. Significant differences are found: 1) The reconnection electric field in the 3D simulation is concentrated at the x-line but is much more diffused in the 2.5D simulation, indicating that in 3D the annihilation rate of magnetic field lines is much higher in the

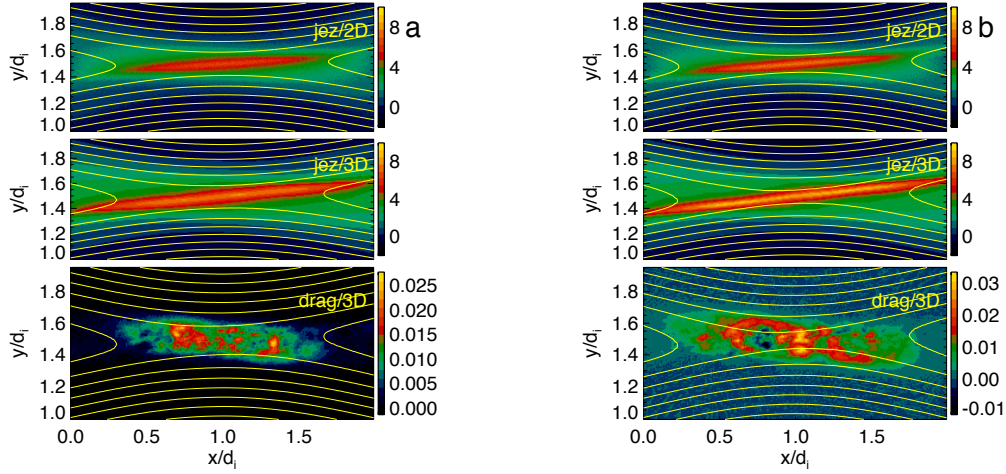


FIG. 5. The top two panels in **a** & **b** show the electron current density j_{ez} in 3D and 2.5D magnetic reconnection, and the bottom panels show the drag D_{ez} . **a**: the onset of Buneman instability at $\Omega_{i0}t = 3$ ($\omega_{pe,0}t = 600$); **b**: the peak of Buneman instability at $\Omega_{i0}t = 3.4$ ($\omega_{pe,0}t = 680$). The solid lines represent the magnetic field.

region around the x-line where the drag is stronger than in regions away from the x-line. Away from the x-line the rate is similar to the mean annihilation rate in the 2.5D simulation, consistent with the fact that the Buneman instability only occurs around the x-line; 2) In the 3D simulation, the profile of $\langle E_z \rangle$ along the x-direction resembles a “wavepacket” centred at the x-line. The spatial scale $\sim 0.1 - 0.2d_i$ is consistent with the Buneman “wavepackets” in the current sheet simulation (c.f. Fig. 1) —implying that the reconnection is mediated by the inhomogeneity of the drag in the thin current sheet and electron-scale magnetic reconnections occurs around the x-line.

As we have shown in the current sheet simulations, an important effect of the electron-scale magnetic reconnection is the enhancement of $\langle B_y \rangle$ by the inhomogeneity of the drag (Fig. 5). We show $\langle B_y \rangle$ at $\omega_{pe,0}t = 680$ in both 2.5D and 3D magnetic reconnections in Fig. 7. The $\langle B_y \rangle$ is $\sim 10\% - 20\%$ higher in 3D than in 2.5D reconnection in the area that extends from the electron diffusion region to the ion diffusion region, and consequently

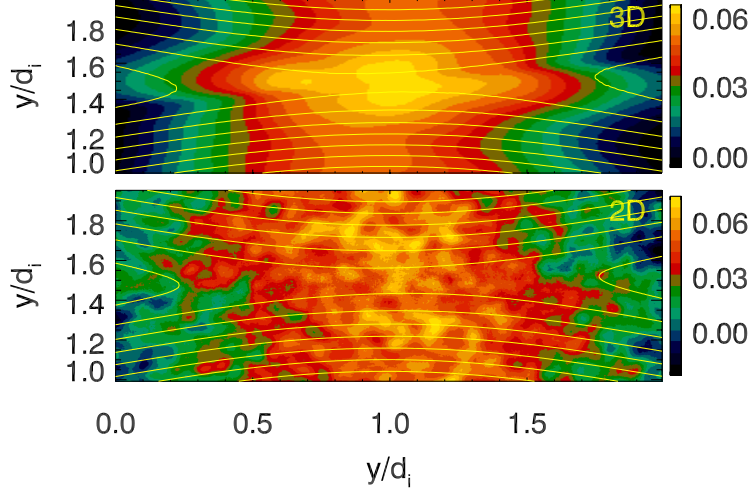


FIG. 6. The reconnection electric field $\langle E_z \rangle$ generated in 3D and E_z in 2.5D magnetic reconnection at the peak of Buneman instability $\Omega_i t = 3.4$ ($\omega_{pe,0} t = 680$). The solid lines are the corresponding magnetic field lines.

increases the opening angle of the magnetic field lines from the x-point. The enhancement of $\langle B_y \rangle$ is asymmetric around the x-point—this is due to the Hall-effect which leads to a quadratic structure of the electron current density in guide magnetic reconnection^{15,19}.

In addition, the enhancement of $\langle E_z \rangle$ and $\langle B_y \rangle$ within the ion diffusion region can lead to the enhancement of the Poynting flux in the x-direction $\langle S_x \rangle = -\frac{c}{4\pi} \langle E_z \rangle \langle B_y \rangle$, where $\langle B_y \rangle = -\partial_x \langle A_z \rangle$ and $\langle E_z \rangle = -\partial_t \langle A_z \rangle$. We show the Poynting flux in Fig. 8. The difference of Poynting flux in 3D and 2.5 D magnetic reconnection follows the asymmetric enhancement of $\langle B_y \rangle$ rather than $\langle E_z \rangle$ which centers at the x-line. The overall increment is about 50-100% which is expected based on the enhancement of $\langle E_z \rangle$ and $\langle B_y \rangle$.

III. CONCLUDING REMARKS

In this paper, we explore how Buneman instability at the x-line accelerates magnetic reconnection with a strong guide field. We show that in a three-dimensional current layer the

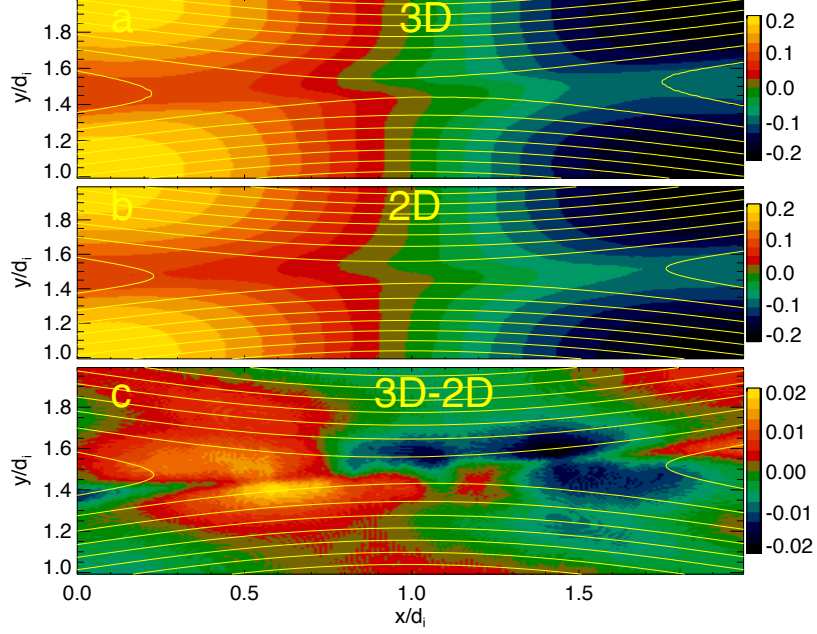


FIG. 7. $\langle B_y \rangle$ generated in 3D and B_y in 2.5D magnetic reconnection at the peak of Buneman instability $\Omega_i t = 3.4$ ($\omega_{pe,0} t = 680$). In bottom panel, the difference between $\langle B_y \rangle$ and B_y is displayed. The magnetic field is shown as solid lines.

dissipation of magnetic energy by AR inevitably leads to fast impulsive electron-scale magnetic reconnections due to the inhomogeneity of drag which generates B_y . The reconnection electric field $\langle E_z \rangle$ peaks at $0.6 B_0 V_A / c$, which is significantly higher than the maximum Hall reconnection rate. We further show that the electron-scale magnetic reconnection produced by Buneman instability at the x-line in a 3D magnetic reconnection has important effects on scales beyond the electron diffusion region. This is because the kinetic turbulence can be transported from the electron diffusion region to ion diffusion by the reconnection outflow. The induced AR not only increases the magnetic reconnection rate at the x-line but also makes the opening angle of magnetic field lines larger in the ion diffusion region. The Poynting flux S_x produced by $-\frac{c}{4\pi} E_z B_y$ is also enhanced in the ion diffusion region of the 3D magnetic reconnection. Our results show that AR produced in the electron diffusion region can couple with Hall effect and increase the reconnection rate.

In a previous study we have shown that Buneman turbulence could facilitate a magnetic

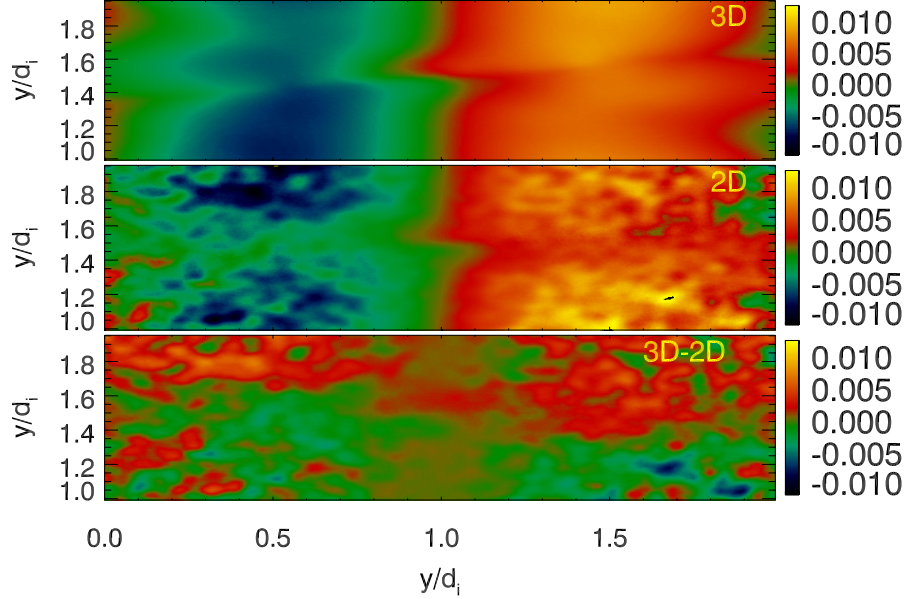


FIG. 8. Poynting flux propagating along x generated in 3D and 2.5D magnetic reconnections at the peak of Buneman instability $\Omega_i t = 3.4$ ($\omega_{pe,0} t = 680$). The bottom panel is the difference of the Poynting flux. The magnetic field is shown as solid lines.

reconnection which is faster than Hall-facilitated reconnection via AR and/or AV. In fact, a group of electron beam instabilities, including Buneman instability, electron two-stream instability⁴⁸ and low hybrid instability⁴⁰ etc, can all develop around the x -line and in the separatrix as the reconnection current sheets proceed to the electron inertia length. These electron electrostatic instabilities can form coherent structures such as electron holes and efficiently dissipate both of the kinetic and magnetic energy via AR. The results reported in this paper shed some new light on the long-standing question: if and how the induced AR or drag surpasses the Hall-effect and accelerates magnetic reconnection process.

The effects discussed, such as electron holes, waves, strong dissipation and pressure anisotropy have direct observational consequences in both magnetospheric and solar coronal current sheets as well as in ion-scale magnetic reconnection in these environments. NASA's *MMS* mission can detect the electron-scale dynamics and is able to observationally determine the role of turbulence in magnetic reconnection^{66,67}.

ACKNOWLEDGMENTS

This research is supported by the NASA *MMS* in association with NASA contract NNG04EB99C. The author thanks the entire *MMS* project for the support, in particular the discussions with colleagues in the FPI team: J. Dorelli, W. Paterson, B. Giles, M. Goldstein, L. Avanov, B. Lavraud, M. Chandler, D. Gershman and C. Schiff, and the participants of 2016 1st MMS community Science Workshop in UCLA. The simulations and analysis were carried out at the NASA Advanced Supercomputing facility at the Ames Research Center and the National Energy Research Scientific Computing Center.

REFERENCES

- ¹C. Robertson, S. W. H. Cowley, and J. W. Dungey, “Wave-particle interactions in a magnetic neutral sheet,” *Planetary and Space Science* **29**, 399–403 (1981).
- ²J. Berchem and C. T. Russell, “The thickness of the magnetopause current layer - ISEE 1 and 2 observations,” *J. Geophys. Res.* **87**, 2108–2114 (1982).
- ³C. T. Russell, X.-W. Zhou, G. Le, P. H. Reiff, J. G. Luhmann, C. A. Cattell, and H. Kawano, “Field aligned currents in the high latitude, high altitude magnetosphere: POLAR initial results,” *Geophys. Res. Lett.* **24**, 1455–1458 (1997).
- ⁴D. E. Wendel and M. L. Adrian, “Current structure and nonideal behavior at magnetic null points in the turbulent magnetosheath,” *J. Geophys. Res.* **118**, 1571–1588 (2013).
- ⁵G. Le, H. Lhr, B. J. Anderson, R. J. Strangeway, C. T. Russell, H. Singer, J. A. Slavin, Y. Zhang, T. Huang, K. Bromund, P. J. Chi, G. Lu, D. Fischer, E. L. Kepko, H. K. Leinweber, W. Magnes, R. Nakamura, F. Plaschke, J. Park, J. Rauberg, C. Stolle, and R. B. Torbert, “Magnetopause erosion during the 17 march 2015 magnetic storm: Combined field-aligned currents, auroral oval, and magnetopause observations,” *Geophys. Res. Lett.* **43**, 2396–2404 (2016), 2016GL068257.
- ⁶H. Karimabadi, V. Roytershteyn, W. Daughton, and Y.-H. Liu, “Recent Evolution in the Theory of Magnetic Reconnection and Its Connection with Turbulence,” *Space Sci. Rev.* **178**, 307–323 (2013).
- ⁷J. A. Klimchuk, “Key Aspects of Coronal Heating,” in *AAS/AGU Triennial Earth-Sun Summit*, AAS/AGU Triennial Earth-Sun Summit, Vol. 1 (2015) p. 203.08.
- ⁸M. Velli, F. Pucci, F. Rappazzo, and A. Tenerani, “Models of coronal heating, turbulence and fast reconnection,” *Philosophical Transactions of the Royal Society of London Series A* **373**, 20140262–20140262 (2015).
- ⁹P. A. Sweet, “The Neutral Point Theory of Solar Flares,” in *IAU Symp. 6: Electromagnetic Phenomena in Cosmical Physics*, edited by B. Lehnert (1958) pp. 123–134.
- ¹⁰J. Birn, J. F. Drake, M. A. Shay, B. N. Rogers, R. E. Denton, M. Hesse, M. Kuznetsova, Z. W. Ma, A. Bhattacharjee, A. Otto, and P. L. Pritchett, “Geospace Environmental Modeling (GEM) magnetic reconnection challenge,” *J. Geophys. Res.* **106**, 3715–3720 (2001).
- ¹¹H. Che, *Non-linear development of streaming instabilities in magnetic reconnection with a strong guide field*, Ph.D. thesis, University of Maryland, College Park (2009).

- ¹²V. M. Vasyliunas, “Theoretical Models of Magnetic Field Line Merging, 1,” *Reviews of Geophysics and Space Physics* **13**, 303–+ (1975).
- ¹³M. Hesse, K. Schindler, J. Birn, and M. Kuznetsova, “The diffusion region in collisionless magnetic reconnection,” *Phys. Plasma* **6**, 1781–1795 (1999).
- ¹⁴M. Hesse, M. Kuznetsova, and M. Hoshino, “The structure of the dissipation region for component reconnection: Particle simulations,” *Geophys. Res. Lett.* **29**, 4–1 (2002).
- ¹⁵J. Birn and E. R. Priest, *Reconnection of magnetic fields : magnetohydrodynamics and collisionless theory and observations* (Reconnection of magnetic fields : magnetohydrodynamics and collisionless theory and observations / edited by J. Birn and E. R. Priest. Cambridge : Cambridge University Press, 2007. ISBN: 9780521854207 (hbk.), 2007).
- ¹⁶M. A. Shay and J. F. Drake, “The role of electron dissipation on the rate of collisionless magnetic reconnection,” *Geophys. Res. Lett.* **25**, 3759–3762 (1998).
- ¹⁷M. A. Shay, J. F. Drake, B. N. Rogers, and R. E. Denton, “The scaling of collisionless, magnetic reconnection for large systems,” *Geophys. Res. Lett.* **26**, 2163–2166 (1999).
- ¹⁸Y. Su, A. M. Veronig, G. D. Holman, B. R. Dennis, T. Wang, M. Temmer, and W. Gan, “Imaging coronal magnetic-field reconnection in a solar flare,” *Nature Physics* **9**, 489–493 (2013).
- ¹⁹T. D. Tharp, M. Yamada, H. Ji, E. Lawrence, S. Dorfman, C. E. Myers, and J. Yoo, “Quantitative Study of Guide-Field Effects on Hall Reconnection in a Laboratory Plasma,” *Phys. Rev. Lett.* **109**, 165002 (2012).
- ²⁰H. Che, J. F. Drake, and M. Swisdak, “A current filamentation mechanism for breaking magnetic field lines during reconnection,” *Nature (London)* **474**, 184 (2011).
- ²¹M. V. Goldman, D. L. Newman, and G. Lapenta, “What Can We Learn about Magnetotail Reconnection from 2D PIC Harris-Sheet Simulations?” *Space Sci. Rev.* **199**, 651–688 (2016).
- ²²R. B. Torbert, J. L. Burch, B. L. Giles, D. Gershman, C. J. Pollock, J. Dorelli, L. Avanov, M. R. Argall, J. Shuster, R. J. Strangeway, C. T. Russell, R. E. Ergun, F. D. Wilder, K. Goodrich, H. A. Faith, C. J. Farrugia, P.-A. Lindqvist, T. Phan, Y. Khotyaintsev, T. E. Moore, G. Marklund, W. Daughton, W. Magnes, C. A. Kletzing, and S. Bounds, “Estimates of terms in Ohm’s law during an encounter with an electron diffusion region,” *Geophys. Res. Lett.* **43**, 5918–5925 (2016).
- ²³L. Fletcher, “Ultra-violet footpoints as tracers of coronal magnetic connectivity and re-

- structuring during a solar flare,” *Astronomy and Astrophysics* **493**, 241–250 (2009).
- ²⁴L. Fletcher, B. R. Dennis, H. S. Hudson, S. Krucker, K. Phillips, A. Veronig, M. Battaglia, L. Bone, A. Caspi, Q. Chen, P. Gallagher, P. T. Grigis, H. Ji, W. Liu, R. O. Milligan, and M. Temmer, “An Observational Overview of Solar Flares,” *Space Sci. Rev.* **159**, 19–106 (2011).
- ²⁵J. Lin, N. A. Murphy, C. Shen, J. C. Raymond, K. K. Reeves, J. Zhong, N. Wu, and Y. Li, “Review on Current Sheets in CME Development: Theories and Observations,” *Space Sci. Rev.* **194**, 237–302 (2015).
- ²⁶M. Øieroset, T. D. Phan, M. Fujimoto, R. P. Lin, and R. P. Lepping, “In situ detection of collisionless reconnection in the Earth’s magnetotail,” *Nature (London)* **412**, 414–417 (2001).
- ²⁷K. Papadopoulos, “A review of anomalous resistivity for the ionosphere.” *Reviews of Geophysics and Space Physics* **15**, 113–127 (1977).
- ²⁸A. Bhattacharjee and E. Hameiri, “Self-consistent dynamolike activity in turbulent plasmas,” *Phys. Rev. Lett.* **57**, 206–209 (1986).
- ²⁹A. A. Galeev, “Reconnection in the magnetotail,” *Space Sci. Rev.* **23**, 411–425 (1979).
- ³⁰P. K. Kaw, E. J. Valeo, and P. H. Rutherford, “Tearing modes in a plasma with magnetic braiding,” *Phys. Rev. Lett.* **43**, 1398–1401 (1979).
- ³¹A. A. Galeev and R. Z. Sagdeev, “Current instabilities and anomalous resistivity of plasma,” in *Basic Plasma Physics: Selected Chapters, Handbook of Plasma Physics, Volume II*, edited by A. A. Galeev and R. N. Sudan (1984) pp. 271–303.
- ³²Z. B. Guo, P. H. Diamond, and X. G. Wang, “Magnetic Reconnection, Helicity Dynamics, and Hyper-diffusion,” *Astrophys. J.* **757**, 173 (2012).
- ³³S. J. Schwartz, E. G. Zweibel, and M. Goldman, “Microphysics in Astrophysical Plasmas,” *Space Sci. Rev.* **178**, 81–99 (2013).
- ³⁴B. Coppi, G. Laval, and R. Pellat, “Dynamics of the Geomagnetic Tail,” *Phys. Rev. Lett.* **16**, 1207–1210 (1966).
- ³⁵B. Coppi and A. B. Friedland, “Processes of Magnetic-Energy Conversion and Solar Flares,” *Astrophys. J.* **169**, 379 (1971).
- ³⁶J. D. Huba, N. T. Gladd, and K. Papadopoulos, “The lower-hybrid-drift instability as a source of anomalous resistivity for magnetic field line reconnection,” *Geophys. Res. Lett.* **4**, 125–126 (1977).

- ³⁷E. N. Parker, “Anomalous resistivity and the evolution of magnetic field topology,” *Astrophys. J.* **414**, 389–398 (1993).
- ³⁸R. M. Kulsrud, “Magnetic reconnection: Sweet-Parker versus Petschek,” *Earth Planet. Space* **53**, 417–422 (2001).
- ³⁹R. A. Treumann, “Origin of resistivity in reconnection,” *Earth, Planets, and Space* **53**, 453–462 (2001).
- ⁴⁰H. Che, J. F. Drake, M. Swisdak, and P. H. Yoon, “Electron holes and heating in the reconnection dissipation region,” *Geophys. Res. Lett.* **37**, 11105–+ (2010).
- ⁴¹P. A. Muñoz and J. Büchner, “Non-Maxwellian electron distribution functions due to self-generated turbulence in collisionless guide-field reconnection,” *Phys. Plasma* **23**, 102103 (2016).
- ⁴²Y. V. Khotyaintsev, D. B. Graham, C. Norgren, E. Eriksson, W. Li, A. Johlander, A. Vaivads, M. André, P. L. Pritchett, A. Retinò, T. D. Phan, R. E. Ergun, K. Goodrich, P.-A. Lindqvist, G. T. Marklund, O. Le Contel, F. Plaschke, W. Magnes, R. J. Strangeway, C. T. Russell, H. Vaith, M. R. Argall, C. A. Kletzing, R. Nakamura, R. B. Torbert, W. R. Paterson, D. J. Gershman, J. C. Dorelli, L. A. Avanov, B. Lavraud, Y. Saito, B. L. Giles, C. J. Pollock, D. L. Turner, J. D. Blake, J. F. Fennell, A. Jaynes, B. H. Mauk, and J. L. Burch, “Electron jet of asymmetric reconnection,” *Geophys. Res. Lett.* **43**, 5571–5580 (2016).
- ⁴³F. D. Wilder, R. E. Ergun, K. A. Goodrich, M. V. Goldman, D. L. Newman, D. M. Malaspina, A. N. Jaynes, S. J. Schwartz, K. J. Trattner, J. L. Burch, M. R. Argall, R. B. Torbert, P.-A. Lindqvist, G. Marklund, O. Le Contel, L. Mirioni, Y. V. Khotyaintsev, R. J. Strangeway, C. T. Russell, C. J. Pollock, B. L. Giles, F. Plaschke, W. Magnes, S. Eriksson, J. E. Stawarz, A. P. Sturmer, and J. C. Holmes, “Observations of whistler mode waves with nonlinear parallel electric fields near the dayside magnetic reconnection separatrix by the Magnetospheric Multiscale mission,” *Geophys. Res. Lett.* **43**, 5909–5917 (2016).
- ⁴⁴R. Nakamura, V. A. Sergeev, W. Baumjohann, F. Plaschke, W. Magnes, D. Fischer, A. Varsani, D. Schmid, T. K. M. Nakamura, C. T. Russell, R. J. Strangeway, H. K. Leinweber, G. Le, K. R. Bromund, C. J. Pollock, B. L. Giles, J. C. Dorelli, D. J. Gershman, W. Paterson, L. A. Avanov, S. A. Fuselier, K. Genestreti, J. L. Burch, R. B. Torbert, M. Chutter, M. R. Argall, B. J. Anderson, P.-A. Lindqvist, G. T. Marklund, Y. V. Khotyaintsev, B. H. Mauk, I. J. Cohen, D. N. Baker, A. N. Jaynes, R. E. Ergun,

- H. J. Singer, J. A. Slavin, E. L. Kepko, T. E. Moore, B. Lavraud, V. Coffey, and Y. Saito, “Transient, small-scale field-aligned currents in the plasma sheet boundary layer during storm time substorms,” *Geophys. Res. Lett.* **43**, 4841–4849 (2016).
- ⁴⁵R. E. Ergun, J. C. Holmes, K. A. Goodrich, F. D. Wilder, J. E. Stawarz, S. Eriksson, D. L. Newman, S. J. Schwartz, M. V. Goldman, A. P. Sturner, D. M. Malaspina, M. E. Usanova, R. B. Torbert, M. Argall, P.-A. Lindqvist, Y. Khotyaintsev, J. L. Burch, R. J. Strangeway, C. T. Russell, C. J. Pollock, B. L. Giles, J. J. C. Dorelli, L. Avanov, M. Hesse, L. J. Chen, B. Lavraud, O. Le Contel, A. Retino, T. D. Phan, J. P. Eastwood, M. Oieroset, J. Drake, M. A. Shay, P. A. Cassak, R. Nakamura, M. Zhou, M. Ashour-Abdalla, and M. Andr, “Magnetospheric multiscale observations of large-amplitude, parallel, electrostatic waves associated with magnetic reconnection at the magnetopause,” *Geophys. Res. Lett.* **43**, 5626–5634 (2016), 2016GL068992.
- ⁴⁶D. B. Graham, Y. V. Khotyaintsev, A. Vaivads, and M. André, “Electrostatic solitary waves and electrostatic waves at the magnetopause,” *J. Geophys. Res.* **121**, 3069–3092 (2016).
- ⁴⁷H. Ji, M. Yamada, S. Hsu, and R. Kulsrud, “Experimental Test of the Sweet-Parker Model of Magnetic Reconnection,” *Phys. Rev. Lett.* **80**, 3256–3259 (1998).
- ⁴⁸H. Che, J. F. Drake, M. Swisdak, and P. H. Yoon, “Nonlinear Development of Streaming Instabilities in Strongly Magnetized Plasma,” *Phys. Rev. Lett.* **102**, 145004–+ (2009).
- ⁴⁹J. F. Drake, M. Swisdak, C. Cattell, M. A. Shay, B. N. Rogers, and A. Zeiler, “Formation of Electron Holes and Particle Energization During Magnetic Reconnection,” *Science* **299**, 873–877 (2003).
- ⁵⁰A. Le, J. Egedal, and W. Daughton, “Two-stage bulk electron heating in the diffusion region of anti-parallel symmetric reconnection,” *Phys. Plasma* **23**, 102109 (2016).
- ⁵¹Y. V. Khotyaintsev, A. Vaivads, M. André, M. Fujimoto, A. Retinò, and C. J. Owen, “Observations of Slow Electron Holes at a Magnetic Reconnection Site,” *Phys. Rev. Lett.* **105**, 165002–+ (2010).
- ⁵²S. Y. Li, Y. Omura, B. Lembège, X. H. Deng, H. Kojima, Y. Saito, and S. F. Zhang, “Geotail observation of counter directed ESWs associated with the separatrix of magnetic reconnection in the near-Earth magnetotail,” *J. Geophys. Res.* **119**, 202–210 (2014).
- ⁵³M. Øieroset, D. Sundkvist, C. C. Chaston, T. D. Phan, F. S. Mozer, J. P. McFadden, V. Angelopoulos, L. Andersson, and J. P. Eastwood, “Observations of plasma waves in

- the colliding jet region of a magnetic flux rope flanked by two active X lines at the subsolar magnetopause,” *J. Geophys. Res.* **119**, 6256–6272 (2014).
- ⁵⁴D. B. Graham, Y. V. Khotyaintsev, A. Vaivads, and M. André, “Electrostatic solitary waves with distinct speeds associated with asymmetric reconnection,” *Geophys. Res. Lett.* **42**, 215–224 (2015).
- ⁵⁵C. Norgren, M. André, A. Vaivads, and Y. V. Khotyaintsev, “Slow electron phase space holes: Magnetotail observations,” *Geophys. Res. Lett.* **42**, 1654–1661 (2015).
- ⁵⁶G. Beskin, S. Karpov, V. Plokhotnichenko, A. Stepanov, and Y. Tsap, “Discovery of the Sub-second Linearly Polarized Spikes of Synchrotron Origin in the UV Ceti Giant Optical Flare,” *the Astronomical Society of Australia* **34**, e010 (2017).
- ⁵⁷A. Zeiler, D. Biskamp, J. F. Drake, B. N. Rogers, M. A. Shay, and M. Scholer, “Three-dimensional particle simulations of collisionless magnetic reconnection,” *J. Geophys. Res.* **107**, 1230–+ (2002).
- ⁵⁸H. Che, J. F. Drake, M. Swisdak, and M. L. Goldstein, “The adiabatic phase mixing and heating of electrons in Buneman turbulence,” *Phys. Plasma* **20**, 061205 (2013).
- ⁵⁹H. Che, “Two-fluid description of wave-particle interactions in strong Buneman turbulence,” **21**, 062305 (2014).
- ⁶⁰B. U. Ö. Sonnerup, “Magnetic Field Reconnection,” in *Space Plasma Physics: The Study of Solar-System Plasmas. Volume 2* (1979) pp. 879–+.
- ⁶¹D. A. Uzdensky and R. M. Kulsrud, “Physical origin of the quadrupole out-of-plane magnetic field in Hall-magnetohydrodynamic reconnection,” *Phys. Plasma* **13**, 062305–062305 (2006).
- ⁶²M. E. Mandt, R. E. Denton, and J. F. Drake, “Transition to whistler mediated magnetic reconnection,” *Geophys. Res. Lett.* **21**, 73–76 (1994).
- ⁶³B. N. Rogers, R. Denton, J. Drake, and M. Shay, “Role of Dispersive Waves in Collisionless Magnetic Reconnection,” *Phys. Rev. Lett.* **87**, 195004 (2001).
- ⁶⁴J. F. Drake, M. A. Shay, and M. Swisdak, “The Hall fields and fast magnetic reconnection,” *Phys. Plasma* **15**, 042306 (2008).
- ⁶⁵G. Lapenta, S. Markidis, A. Divin, M. Goldman, and D. Newman, “Scales of guide field reconnection at the hydrogen mass ratio,” *Phys. Plasma* **17**, 082106 (2010).
- ⁶⁶J. L. Burch, T. E. Moore, R. B. Torbert, and B. L. Giles, “Magnetospheric Multiscale Overview and Science Objectives,” *Space Sci. Rev.* **199**, 5–21 (2016).

⁶⁷T. D. Phan, J. P. Eastwood, P. A. Cassak, M. Øieroset, J. T. Gosling, D. J. Gershman, F. S. Mozer, M. A. Shay, M. Fujimoto, W. Daughton, J. F. Drake, J. L. Burch, R. B. Torbert, R. E. Ergun, L. J. Chen, S. Wang, C. Pollock, J. C. Dorelli, B. Lavraud, B. L. Giles, T. E. Moore, Y. Saito, L. A. Avanov, W. Paterson, R. J. Strangeway, C. T. Russell, Y. Khotyaintsev, P. A. Lindqvist, M. Oka, and F. D. Wilder, “MMS observations of electron-scale filamentary currents in the reconnection exhaust and near the X line,” *Geophys. Res. Lett.* **43**, 6060–6069 (2016).